J Therm Anal Calorim (2010) 100:577–587
DOI 10.1007/s10973-009-0512-7

Studies of Co(II), Ni(II), Cu(II) and Cd(II) chelates with different phosphonic acids

B. Venkateswara Rao

Received: 7 April 2009 / Accepted: 22 September 2009 / Published online: 11 November 2009

Abstract Co(II), Ni(II), Cu(II) and Cd(II) chelates with 1-aminoethylidenediphosphonic acid (AEDP, H_4L^1), zα-amino benzylidene diphosphonic acid (ABDP, H_4L^2), 1-amino-2-carboxyethane-1,1-diphosphonic acid (ACEDP, H_5L^3), 1,3-diaminopropane-1,1,3,3-tetraphosphonicacid (DAPTP, H_8L^4), ethylenediamine-*N*,*N*′-bis(dimethylmethylene phosphonic)acid (EDBDMPO, H_4L^5), *O*-phenylenediamine-*N*,*N*′-bis(dimethyl methylene phosphonic)acid (PDBDMPO, H_4L^6), diethylene triamine-*N*,*N*,*N*′,*N*′,*N*″*N*″-penta(methylene phosphonic)acid (DETAPMPO, $H_{10}L^7$) and diethylene triamine-*N*,*N*″-bis(dimethyl methylene phosphonic)acid (DETBDMPO, H_4L^8) have been synthesised and were characterised by elemental and thermal analyses as well as by IR, UV–VIS, EPR and magnetic measurements. The first stage in the thermal decomposition process of these complexes shows the presence of water of hydration, the second denotes the removal of the coordinated water molecules. After the loss of water molecules, the organic part starts decomposing. The final decomposition product has been found to be the respective $MO{\cdot}P_2O_5$. The data of the investigated complexes suggest octahedral geometry with respect to Co(II) and Ni(II) and tetragonally distorted octahedral geometry with respect to Cu(II). Antiferromagnetism has been inferred from magnetic moment data. Infrared spectral studies have been carried out to determine coordination sites.

B. V. Rao (✉)
Department of Chemistry, Andhra Loyola College (Autonomous), Vijayawada, Andhra Pradesh, India
e-mail: bvrsss@yahoo.co.in

Keywords Antiferromagnetism · Metal phosphonic acid chelates · Octahedral geometry · Phosphonic acid · Thermal decomposition

Introduction

On the basis of structural examination, organophosphonic acids possessed potentialities for complex formation. These organoaminophosphonic acids contained two highly acidic phosphono groups and a hydroxy or amino group which played the role of the basic centre in the molecule, enabling these ligands to form more stable complexes. Aminoethylidenediphosphonic acid (AEDP) and α-amino benzylidenediphosphonic acid (ABDP) had a very strong herbicidal effect against barnard grass, mustard and tomato seedlings and had fungicidal properties [1–3]. One can use 1-amino-2-carboxyethane-1,1-diphosphonic acid (ACEDP) as water softener, for flask cleaning or as additive for dyeing baths for textiles [4, 5]. Alkylenebisnitrilodialkylphosphonic acid forms very stable complexes with bivalent metal that lead to the elimination of metal from the organism [6]. EDBDMPO and DETAPMPO have been found to be more effective than DTPA (diethylene triamine penta acetic acid) in reducing the uranium content in rat organs [7, 8]. Polyaminealkylphosphonic acids may be used as effective ligands for binding and eliminating uranium and its fission products from the body [9, 10].

From the survey of the literature above on the study of some organophosphonic acids and their metal derivatives, it is evident that except for the physico-chemical and biological studies, very little work seems to have been carried out on the synthetic and structural aspects of metal derivatives of organo aminophosphonic acids. In view of this, it was thought of interest to attempt the studies of

Co(II), Ni(II), Cu(II) and Cd(II) chelates with different phosphonic acids.

Experimental

Materials and methods

All chemicals used were of AnalaR or reagent grade. 1-amino ethylidene di-phosphonic acid (AEDP, H_4L^1) was prepared by the reaction reported by Ploger et al. [11] reacting acetamide with phosphorus trichloride and diethylphosphite in 1:3:1 molar ratio. α-Amino benzylidene diphosphonic acid (ABDP, H_4L^2), 1-amino-2-carboxyethane-1,1-diphosphonic acid (ACEDP, H_5L^3) and 1,3-diaminopropane-1,1,3,3-tetraphosphonic acid (DAPTP, H_8L^4) were prepared by the method used by Lerch and Kottler [12, 13]. Ethylenediamine-*N*,*N*′-bis(dimethyl methylenephosphonic)acid (EDBDMPO, H_4L^5), and *O*-phenylenediamine-*N*,*N*′-bis(dimethylmethylenephosphonic)acid (PDBDMPO, H_4L^6), have been prepared by the method reported by Kabachnik et al. [14–21]. Diethylene triamine-*N*,*N*,*N*′,*N*′,*N*″*N*″-penta(methylene phosphonic)acid (DETAPMPO, $H_{10}L^7$) has been prepared by the method used by Peck and Hudson [22, 23]. Diethylene triamine-*N*,*N*″-bis(dimethyl methylene phosphonic)acid (DETBDMPO, H_4L^8) have been prepared in aqueous medium by the method reported by Medved et al. [24].

Preparation of metal derivatives of phosphonic acids [25]

1. $Co_2(L^1)\cdot 3H_2O$ complex: To 0.001 mole of ligand in water was added 0.002 mole of aq. cobalt(II) acetate solution. It was followed by addition of 20 ml of 0.004 M aq. NaOH solution. On addition of acetone to this, a violet precipitate settled down. The precipitate was filtered, washed several times with hot water, aq. acetone and finally with acetone (90%). It was then dried on water bath at about 60 °C. Yield is 80%
2. $Ni_2(L^2)\cdot 2H_2O$ complex: 0.002 mole of aq. nickel(II) acetate solution was slowly introduced into 0.001 mole of ligand in water while stirring continuously. A light green solid separated and settled in the solution. The yield was increased by the addition of acetone. The precipitate was filtered, washed several times with water, aqueous acetone and acetone (90%). It was then dried at about 50–60 °C. Yield is 80%.
3. $Co_5(L^3)_2\cdot 2H_2O$ complex: To 10 ml of 0.001 M aq. ligand solution was added 10 ml of 0.0025 M aq. Na_2CO_3 solution. This was followed by the addition of 10 ml of 0.0025 M aq. cobalt(II) acetate solution. The solution was stirred throughout this process. Light violet precipitate was formed. Acetone was also added when further precipitation occurred. The violet coloured solid after filtration was given washings with hot water till the filtrate was colourless, then with aqueous acetone and finally with 90% acetone. It was then dried in an air oven at 76–80 °C. Yield is 69%.
4. $Ni_5(L^3)_2\cdot 5H_2O$ complex: The same procedure given in 3 was adopted and instead of cobalt(II) acetate, nickel(II) acetate was taken. Yield is 67%.
5. $Cu_5(L^3)_2\cdot 5H_2O$ complex: The same procedure given in 3 was adopted and instead of cobalt(II) acetate, copper(II) acetate was taken. Yield is 65%.
6. $Co_4(L^4)\cdot 11H_2O$ complex: To 10 ml of 0.1 M aq. ligand solution was added 40 ml of 0.1 M aq. Na_2CO_3 solution. This was followed by 40 ml of 0.1 M aq. cobalt(II) acetate solution. A purple-coloured precipitate settled down. The precipitate was filtered, washed several times with hot water, aqueous acetone and acetone (90%). It was then dried on water bath. Yield is 80%.
7. $Ni_2(L^5)\cdot 4H_2O$ complex: To an aqueous solution of 0.002 mole of the ligand was added an aqueous solution of 0.004 mole nickel(II) acetate drop wise and with constant stirring. A transparent green layer was obtained which was separated first in a separating funnel and then washed with alcohol for solidification. At once, a light green solid compound was formed. The precipitate was filtered, washed with hot water, 50% acetone and finally acetone (90%) and then dried at 60–70 °C. The yield of light green solid is 91%.
8. $Ni_2(L^6)\cdot 2H_2O$ complex: The same procedure given in 7 was adopted. Yield is 75%.
9. $Ni_5(L^7)\cdot 20H_2O$ complex: To 50 ml of 0.1 M aq. nickel(II) acetate solution, 10 ml of the ligand (0.1 M) solution was added and then 25 ml of 0.1 M aq. Na_2CO_3 solution was introduced drop wise with constant stirring. A light green-coloured precipitate was obtained which was filtered, washed with hot water, aqueous acetone, and acetone and then finally dried on water bath. Yield is 81%.
10. $Cd_2(L^8)\cdot 3H_2O$ complex: 0.0025 mole of the ligand was dissolved in water and to it was added 10 ml of 1 M (0.01 mole) solution of NaOH. When 0.005 mole of cadmium(II) acetate was added to the above mixture solution, a white precipitate was formed. The precipitate was filtered, washed with hot water, aqueous acetone, acetone (90%) and dried on water bath. Yield is 87%.

Carbon and hydrogen in case of ligands were estimated by means of semi-micro analyzer, LG, VEB Laborgerate and Orthopadic Leipzig. Nitrogen was estimated by Duma's method. Metal and phosphorus contents were determined by standard procedures [26].

Physical measurements

Diffused transmittance spectra were run on DMR-21 spectrophotometer in 200–2,000 nm (50,000–5,000 cm^{-1}) region. Diffused reflectance spectra were run on Cary 2390 spectrophotometer in 200–1,800 nm (50,000–5,555.5 cm^{-1}) region at RSIC, Madras, India. Magnetic susceptibility measurements were carried out using a Princeton Applied Research Model 155 Vibrating Sample Magnetometer incorporating a digital read out. The electromagnet was fed from a polytronic constant current regulator (Type CP 200). A pure nickel pellet was used as calibrant, cross checking against $Hg[Co(CNS)_4]$. The instruments and methods used for the remainder of the analyses were the same as described earlier [27–29]. Thermal analysis of the compounds was done in the atmosphere of air at National Chemical Laboratory, Pune, India. The specimens were heated at the rate of 10 °C/min in 20–1,000 °C range and heated alumina was used as standard.

Results and discussion

Infrared spectra

Infrared spectra of the free ligand, a characteristic band is observed at 1,190 cm^{-1} (AEDP, H_4L^1), 1,230 cm^{-1} (ABDP, H_4L^2), 1,160 cm^{-1} (ACEDP, H_5L^3), 1,160 cm^{-1} (DAPTP, H_8L^4), 1,220 cm^{-1}(EDBDMPO, H_4L^5), 1,210 cm^{-1} (PDBDMPO, H_4L^6), 1,240 cm^{-1} DETAPMPO, $H_{10}L^7$), 1,190 cm^{-1} (DETBDMPO, H_4L^8), which may be due to the phosphoryl ν(P=O) vibrations. Żurowska et al. [30] have assigned 1,260–1,160 cm^{-1} region for ν(P=O) stretching frequency from the survey of a large number of phosphorus compounds having free phosphoryl group. Stretching vibrations of phosphoryl group in case of metal derivatives have been observed at 1,110–1,155 cm^{-1}. The displacement of the band by 45–90 cm^{-1} towards lower region has been attributed to the formation of coordination bond between phosphoryl oxygen and metal ion [27–34]. The two more bands at around 1,130 and around 1,020 cm^{-1} were observed in all the free ligands correspond to $\nu_{as}PO_2$ and ν_sPO_2 vibrations in HPO_3^{-1} group. In addition, ν_{as}P–OH and ν_sP–OH bands, corresponding to P–$(OH)_2$ also appeared at around 1,000 and around 940 cm^{-1}. In metal derivatives, the asymmetric and symmetric mode of stretching vibration of PO_3 group appeared at 1,070–1,020 and 1,000–900 cm^{-1} ranges, respectively, and splitting of these bands was observed. Such splitting is expected in view of the covalent character of M–O bond due to lowering of the symmetry of PO_3^{-2} group. In case of AEDP and ABDP, the stretching and bending mode of $-NH_3^+$ group have been observed at 3,400 and 1,580 cm^{-1}, respectively. The bands at 3,400 and 3,200 cm^{-1} may be due to the presence of OH/NH groups. Two more bands at 3,060 and 1,450 cm^{-1} were present in ABDP and may be assigned due to aromatic grouping [35]. In the infrared spectra of complexes, the rocking and wagging vibrations appeared in the regions 880–860 and 750–710 cm^{-1} suggesting the presence of coordinated water [36–38].

A medium sharp band due to $\nu_{as}(COO^-)$ group observed at 1,660 cm^{-1} in the free ligand (ACEDP), shifted to lower frequency (1,645–1,630 cm^{-1}) in all the complexes indicating that the carboxylic group is coordinated to the metal atom of the same or another molecule. Another band found at 1,300 cm^{-1} in the free ligand (ACEDP) spectrum was due to the presence of $\nu_{as}(COO^-)$ vibration. In the metal complexes, this band was found shifted to 1,430–1,400 cm^{-1} indicating the involvement of the carboxylic group in bond formation with the metal [39]. The lowering of $\nu_{as}(COO^-)$ (mainly due to ν(C=O) of the (COOH group)) and the difference $\Delta = \nu_{as}(COO^-) - \nu_s(COO^-)$ is approximately equal to 200 cm^{-1} clearly suggested the coordinations of ν(C=O) moiety to the metal atom [39–42]. The bands at 1,090 and 1,040 cm^{-1} were assigned to $\nu_{as}(PO_2)$ and $\nu_s(PO_2)$ vibrations in the group HPO_3^-. Two more bands were observed at 990 and 940 cm^{-1} that may be due to ν_{as}P–$(OH)_2$ and ν_sP–$(OH)_2$ vibrations of PO_3H_2 group in case of DETBDMPO. NH_2^+ group often gives two broad unresolved bands in the region of 3,000–2,750 cm^{-1}. In the infrared spectrum of free DETBDMPO, there was a broad band in the region 3,400–2,600 cm^{-1} which may be due to masking of $\nu(NH_2^+)$ bands by broad ν(OH) band. A weak band at 1,620 cm^{-1} has been assigned to ν(N–H) [35, 43]. Two bands were present in the region of 450–410 cm^{-1} and 330–300 cm^{-1} in far infrared spectra of complexes and assigned to M–O and M–N linkages, respectively [44, 45].

Electronic spectra

1. $Co_2(L^1)\cdot 3H_2O$ complex: The blue violet complex showed electronic spectrum typical of six-coordinated complexes [46–56]. The absorption bands have been observed at 8,160 (16,390), 17,540 and 20,000 cm^{-1} for $Co_2(L^1)\cdot 3H_2O$ complex and assignment for these bands are due to the excited state terms $^4T_2g(F)$, $^4A_2g(F)$ and $^4T_1g(P)$, respectively, from the ground term $^4T_1g(F)$. The frequency on visible band at 16,390 cm^{-1} can arise through low symmetry components to the ligand field or

through the presence of spin-forbidden transitions made evident by intensity stealing from the allowed band. The splitting of near infrared bands to 7,170 and 8,160 cm^{-1} reveals the presence of low symmetry components to the ligand field.

2. $Co_5(L^3)_2{\cdot}2H_2O$ complex: The $Co_5(L^3)_2{\cdot}2H_2O$ complex exhibited three main absorption bands at 10,420, 17,860 (19,230) and 27,780 cm^{-1} in its electronic spectrum due to the transition $^4T_2g(F)(v_1)$, $^4A_2g(F)(v_2)$ and $^4T_1g(P)(v_3)$, respectively, arising from the ground state $^4T_1g(F)$. They have been assigned to the formation of an octahedral complex [45]. The band v_2 splits into two bands (17,860 and 19,230 cm^{-1}). A shoulder at 14,290 cm^{-1} was also observed [46–56].
3. $Co_4(L^4){\cdot}11H_2O$ complex: Absorption bands at 10,640, 16,260 (18,020) and 23,700 cm^{-1} for $Co_4(L^4){\cdot}11H_2O$ were assigned, respectively, to $^4T_1g(F) \leftarrow {}^4T_2g(F)(v_1)$, $^4T_1g(F) \leftarrow {}^4A_2g(F)(v_2)$ and $^4T_1g(F) \leftarrow {}^4T_1g(P)(v_3)$ transitions for octahedral geometry [46–56]. In addition to this, two more bands were observed at 13,510 and 13,590 cm^{-1} in the spectra of the two complexes, respectively. These may be due to spin-forbidden transitions [46–50].
4. $Ni_2(L^2){\cdot}2H_2O$ complex: The light green colour six-coordinated Ni(II) complex gave three bands at 8,300, 13,890 and 25,640 cm^{-1} in its electronic spectrum which can be assigned to $^3T_2g(F) \leftarrow {}^3A_2g(F)(v_1) \leftarrow {}^3T_1g(F){}^3A_1g(F)(v_2)$ and $^3T_1g(F) \leftarrow {}^3A_2g(F)$ (v_3), respectively. There are also some weak bands in the region of 15,000–18,000 cm^{-1} at 15,630 and 17,390 cm^{-1} that may be attributed to spin-forbidden transitions. Octahedral geometry [46–50] has been assigned based on three spin-allowed transitions. The spin-forbidden transition could be interpreted in terms of spin–orbit coupling.
5. $Ni_5(L^3)_2{\cdot}5H_2O$ complex: The diffused reflectance spectrum of the light green $Ni_5(L^3)_2{\cdot}5H_2O$ complex exhibited three absorption bands at 10,990, 16,950 and 25,970 cm^{-1} which may be due to v_1, v_2 and v_3 transitions, respectively, suggesting octahedral geometry [47–58]. In addition, one spin-forbidden transition was observed at 12,500 cm^{-1} $^1Eg \leftarrow {}^3A_2g$.
6. $Ni_2(L^5){\cdot}4H_2O$ complex: Three absorption bands at 8,370, 14,290 and 25,640 cm^{-1} for the light green $Ni_2(L^5){\cdot}4H_2O$ complex have been observed for v_1, v_2 and v_3 transitions, suggesting octahedral geometry [42, 46–58].

$$8,370\ cm^{-1} \quad {}^4A_2g(F) \leftarrow {}^4T_2g(F)(v_1)$$

$$14,290\ cm^{-1} \quad {}^4A_2g(F) \leftarrow {}^{3T_1}\ g(F)(v_2)$$

$$25,640\ cm^{-1} \quad {}^4A_2g(F) \leftarrow {}^{3T_1}\ g(F)(v_3)$$

7. $Ni_2(L^6){\cdot}2H_2O$ complex: The electronic spectrum of nickel complex shows first two bands at 8,300 and 13,890 cm^{-1} and third one at 25,320 cm^{-1} which correspond to the transitions $^3A_2g \leftarrow {}^3T_2g(F)(v_1)$, $^3A_2g \leftarrow {}^3T_1g(F)(v_2)$ and $^3A_2g \leftarrow {}^3T_1g(P)(v_3)$, respectively. These results are in agreement with those observed for Ni(II) octahedral complexes for d^8 configuration [42, 46–58].
8. $Ni_5(L^7){\cdot}20H_2O$ complex: The electronic spectrum gave three main absorption bands at 10,530 cm^{-1} for $^4A_2g(F) \leftarrow {}^3T_2g(F)(v_1)$ at 18,350 cm^{-1} for $^4A_2g(F) \leftarrow {}^3T_1g(F)(v_2)$ and at 30,300 cm^{-1} for $^4A_2g(F) \leftarrow {}^3T_1$ $g(F)(v_3)$ transitions assigned for octahedral geometry. Four more bands were observed at 14,710, 16,950, 20,830 and 33,900 cm^{-1} as shoulders [42, 46–58].
9.. $Cu_5(L^3)_2{\cdot}4H_2O$ complex: For copper(II)–ACEDP complex $(Cu_5(L^3)_2{\cdot}4H_2O)$ a band at 20,000 cm^{-1} has been attributed to the transition $^2E_g \leftarrow {}^2T_{2g}$ which is typical of Cu(II) ion in the tetragonally distorted octahedral environment [52, 53]. Some authors have attributed this to a ligand field band.

Magnetic moments (Tables 1, 2)

1. $Co_2(L^1){\cdot}3H_2O$ complex: The magnetic properties of high spin octahedral cobalt(II) complexes were governed by the partially degenerate ground term ^4T_1g. This provides an orbital contribution to the magnetic moment. Therefore, the room temperature magnetic moments should be in the 4.30–5.20 B.M. range. However, magnetic moment value for $Co_2(L^1){\cdot}3H_2O$ complex has been found to be at 3.43 B.M. indicating that antiferromagnetic interactions may be operative [59–63].
2. $Co_5(L^3)_2{\cdot}2H_2O$ complex: The complex has the magnetic moment 3.0 B.M. at nearly room temperature (306 K), compared to the normal moments of 4.30–5.20 B.M. expected for d^7 spin-free complexes, presumably due to the presence of an appreciable amount of antiferromagnetic property [59–63]. Aggarwal et al. [64] have reported that due to the partial oxidation of the central metal atom to the higher oxidation state also, the lowering of magnetic moment value takes place. This possibility in case of cobalt(II) in the present investigation was ruled out because the magnetic moment of the complexes was not effected even when kept in air for long (10 to 20 days).
3. $Co_4(L^4){\cdot}11H_2O$ complex: The magnetic moment value of $Co_4(L^4){\cdot}11H_2O$ complex has been found to be 2.5 B.M, at room temperature. Ali Ei-Dssouky et al. [65] have also reported this type of antiferromagnetic nature for their Co(II) complexes with 2-picolyl and 2-lutidyl-methyl ketones. θ value of $-44°$ and $-39°$,

respectively, was reported by the authors [65]. Recently, Andrew [66] and Ball [67] et al. have suggested spin–spin interaction between Co^{+2} ions bridged by some dichelating agents containing conjugated systems. In case of $Co_2H_4L{\cdot}10H_2O$, the values decrease with decreasing temperature from 4.71 B.M. at 296 k to 3.98 B.M. at 77 K. Graph of $1/\chi'M$ versus temperature for the Co_2H_4L complex reported in this work gave a straight line showing a negative value of $\theta = -78°$ [59, 60]. Bhatnagar et al. [68, quoted from 69] have reported negative value of θ for their Co(lactate)$_2$ complex at 300°.

4. $Ni_2(L^2){\cdot}2H_2O$ complex: The magnetic moment value of $Ni_2(L^2){\cdot}2H_2O$ complex has been found to be 2.50 B.M. The low value compared to the spin-only value of 2.83 B.M. (2.80–3.5 B.M.) was attributed to antiferromagnetism [25].
5. $Ni_5(L^3)_2{\cdot}5H_2O$ complex: The observed lower magnetic moment values of the complex (2.8 B.M. at 306 K), compared to that expected for a normal spin-free nickel(II) complex (2.8–3.5 B.M.), and may be due to similar interactions as mentioned in earlier cases.
6. $Ni_2(L^5){\cdot}4H_2O$ complex: The magnetic moment value of 2.63 B.M. is lower than the expected value as compared to the spin-only value of 2.83 B.M. is attributed to antiferromagnetism [25].
7. $Ni_2(L^6){\cdot}2H_2O$ complex: The complex has magnetic moment of 2.67 B.M. at room temperature (298 K), required spin-only value being 2.8 B.M for d^8 system suggesting some antiferromagnetic property [25] and octahedral structure.
8. $Ni_5(L^7){\cdot}20H_2O$ complex (Tables 1, 2): Magnetic moment of $Ni_5(L^7){\cdot}20H_2O$ complex exhibits 1.61 B.M. at 300 K(2.8 B.M. expected for d^8 system) which drops to 1.39 B.M. at 77 K. This suggests the presence of antiferromagnetism ($\theta = -34°$) [64, 65] in the complex [25].
9. $Cu_5(L^3)_2{\cdot}4H_2O$ complex: The magnetic moment value of 0.95 B.M. at 306 K was much lower than the normal value (1.7–2.2 B.M.) for d^9 species and may be due either to metal–metal interaction or super exchange. At 296 K, the magnetic moment value was found to be 0.92 B.M., which further decreased to 0.69 B.M. with decrease in temperature to 77 K. This is also expected for antiferromagnetic complexes [70–72]. Plotting the graph of $1/\chi'M$ versus temperature gave a straight line, a negative value of θ (−100°) was obtained.

Table 1 Temperature dependent magnetic moment data of nickel–DETAPMPO complex

T/K	μ_{eff} /B.M. for $Ni_5(L^7){\cdot}20H_2O$ complex
296	1.575
261	1.568
237	1.564
213	1.562
189	1.552
165	1.517
141	1.499
117	1.469
93	1.434
77	1.408

Thermal analyses

1. $Co_2(L^1){\cdot}3H_2O$ complex (Fig. 1): In case of the cobalt(II) phosphonate, the endothermic effect at 140 °C on DTA curve corresponds to the loss of three molecules of water. The total experimental mass loss of 23% at the formation of metal oxide and P_2O_5 [27–29, 32, 33] is corroborated by the expected loss of 21.73%.
2. $Co_5(L^3)_2{\cdot}2H_2O$ complex (Fig. 2): In this case, the endothermic effect on the DTA curve at 170 °C showed the loss of two water molecules (experimental loss, 8%; theoretical, 8.08%) The next endothermic effect was observed at 240 °C which may be due to the loss of two molecules of ammonia and two molecules of CO_2, corresponding to the mass loss of 15%, the theoretical being 14.95%. Heating it further affects the organic part, which starts decomposing. This decreases the mass further by 19%, the expected theoretical mass loss at this stage being 19.06% for the end product cobalt oxide and phosphorus pentoxide. Similar results have also been observed in case of other organophosphonic acid complexes and rare earths metal complexes of 1-hydroxy ethylidene diphosphonic acid. [27–29, 32, 33].
3. $Co_4(L^4){\cdot}11H_2O$ complex (Fig. 3): In this case, the first endothermic effect at 120 °C on DTA curve shows the loss of six water molecules (experimental loss in mass, 13.76%; theoretical, 13.17%). The second endothermic effect was observed at 480 °C which may be due to the loss of rest of the water molecules, corresponding to mass loss of 24.96% (theoretical, 24.15%). At 555 °C, the third endothermic effect was observed indicating the loss of one molecule of ammonia. The corresponding loss in mass on TG is 25.69% (theoretical, 26.22%). Further heating effects the organic part which starts decomposing, forming the end product $4CoO{\cdot}P_2O_5$ and

Table 2 Analytical and magnetic moment data of metal derivatives of phosphonic acids

Complex	Colour	Found (Calcd.)/%		Magnetic moment μ_{eff}/B.M.
		Metal	*P*	
1. $Co_2(L^1)\cdot 3H_2O$	Violet	30.59 (31.61)	16.25 (16.63)	3.43
2. $Ni_2(L^2)\cdot 2H_2O$	Light green	28.64 (28.19)	15.35 (14.89)	2.5
3. $Co_5(L^3)_2\cdot 2H_2O$	Light violet	35.60 (35.99)	15.01 (15.15)	3.00
4. $Ni_5(L^3)_2\cdot 5H_2O$	Light green	32.90 (33.68)	14.11 (14.23)	2.20
5. $Cu_5(L^3)_2\cdot 4H_2O$	Light blue	35.62 (33.68)	13.90 (14.13)	0.95[a]
				0.92[b]
6. $Co_4(L^4)\cdot 11H_2O$	Purple	28.99 (28.75)	15.56 (15.13)	2.50
7. $Ni_2(L^5).4H_2O$	Light green	24.6 (23.99)	13.0 (12.67)	2.63
8. $Ni_2(L^6)\cdot 2H_2O$	Light green	23.9 (23.41)	12.6 (12.37)	2.67
9. $Ni_5(L^7)\cdot 20H_2O$	Light green	24.51 (24.13)	13.04 (12.74)	1.61
10. $Cd_5(L^7)\cdot 16H_2O$	White	40.01 (39.77)	11.04 (10.97)	
11. $Cd_2(L^8)\cdot 3H_2O$	White	35.92 (36.15)	9.8 (9.97)	

[a] 306 K

[b] 296 K

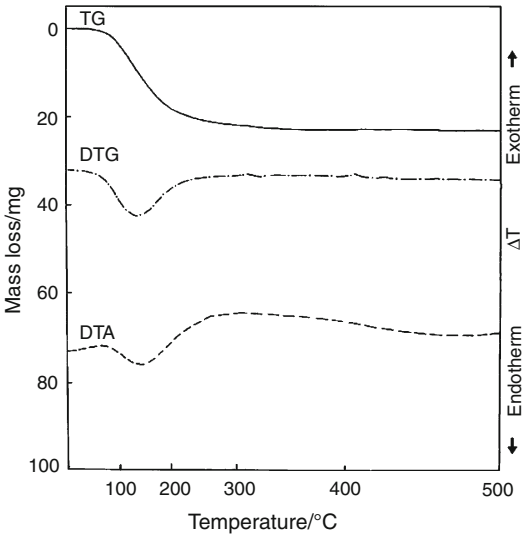

Fig. 1 Thermoanalytical curves of $Co_2(C_2H_5NO_6P_2)\cdot 3H_2O$ (100 mg specimen)

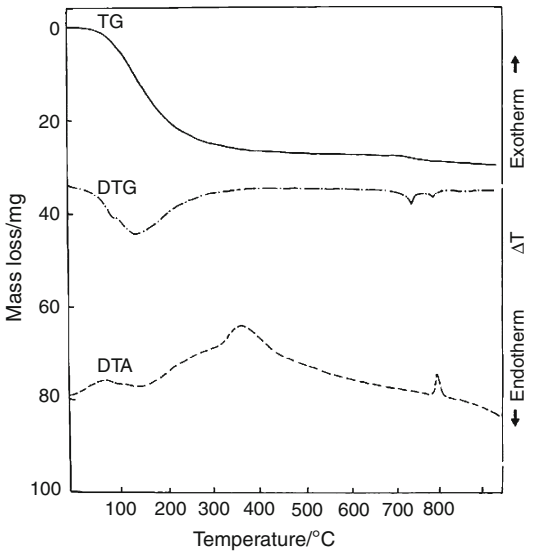

Fig. 2 Thermoanalytical curves of $Co_5(C_3H_4NO_8P_2)_2\cdot 2H_2O$ (100 mg specimen)

requiring a theoretical mass loss of 28.78% (experimental, 29.36%). Similar results have also been observed in case of other organophosphonic acids complexes and rare earth metal complexes of 1-hydroxyethylidenediphosphonic acid [27–29, 32, 33].

4. $Ni_2(L^2)\cdot 2H_2O$ complex (Fig. 4): In this case, the endothermic effects at 100 and 125 °C on the DTA curve for $Ni_2(L^2)\cdot 2H_2O$ complex correspond to the consecutive loss of first and second water molecules, respectively. Two exothermic affects at 370 and 800 °C were observed on DTA curve. The corresponding mass loss in TG is 26 and 29%, respectively. However, no definite stages of decomposition could be identified after the total loss of water molecules from the complex compound suggesting that now the organic part starts decomposing. The final product is $2NiO\cdot P_2O_5$ as inferred from total experimental mass loss of 29.9% (theoretical, 30%) of the complex. The formation of the final product of this type has also been reported by Khramov et al. [33] for their rare earths organophosphonic acids complexes as well as from some other organophosphonic acid complexes [27–29].
5. $Ni_5(L^3)_2\cdot 5H_2O$ complex (Fig. 5): The thermo analytical curves of $Ni_5(L^3)_2\cdot 5H_2O$ complex suggests that five molecules of water were lost in a single step with

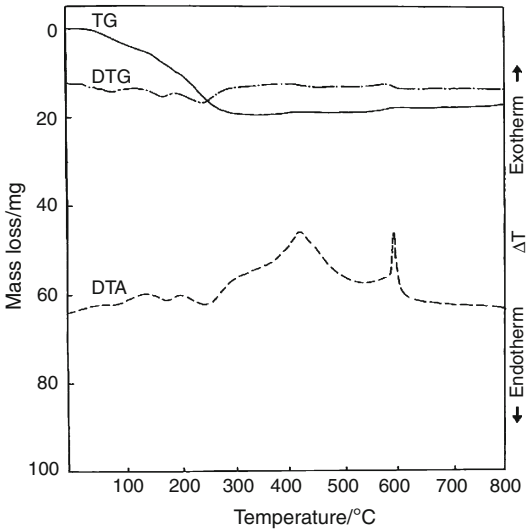

Fig. 3 Thermoanalytical curves of $Co_4(C_3H_6N_2O_{12}P_4)\cdot 11H_2O$ (109 mg specimen)

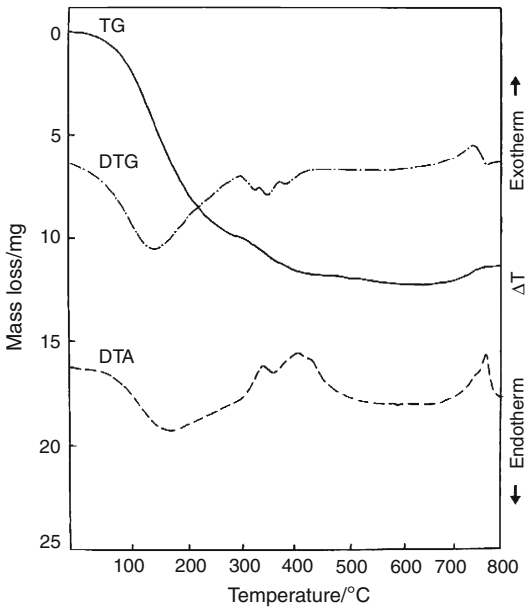

Fig. 4 Thermoanalytical curves of $Ni_2(C_7H_7NO_6P_2)\cdot 2H_2O$ (100 mg specimen)

the corresponding endothermic effect at 154 °C (theoretical loss in mass, 10.33%; observed, 10.5%). Then two molecules of NH_3 and two of CO_2 were lost when heated up to 180 °C. No definite stages of decomposition could further be distinguished positively. However, the DTG curve indicated a decomposition stage between 300 and 405 °C. The corresponding mass loss up to 405 °C is 23%. It seems that after the total loss of water molecules, the organic moiety starts decomposing with the formation of end product, 5 $NiO\cdot P_2O_5$

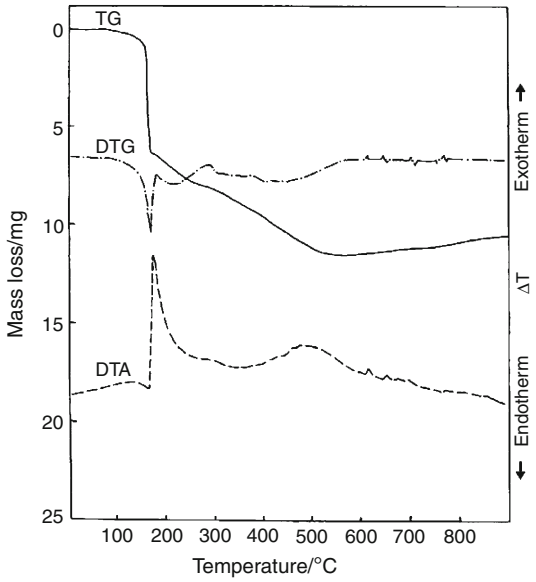

Fig. 5 Thermoanalytical curves of $Ni_5(C_3H_4NO_8P_2)_2\cdot 5H_2O$ (200 mg specimen)

[27–29, 32, 33]. It requires a theoretical mass loss of 23.56% (experimental, 24.5%).

6. $Ni_2(L^5)\cdot 4H_2O$ complex (Fig. 6): The mass loss DTA curve in the thermo analytical curves of $Ni_2(L^5)\cdot 4H_2O$ complex at 100 and 180 °C correspond to 7.5 and 15%, respectively. Decomposition stages could only be detected on the DTG curve between 280 and 340 °C, and between 600 and 720 °C. The TG curve, corresponding to these temperatures, showed mass losses of 27.5 and 37.5% having exothermic peaks at 310, 370, 630 and 690 °C, respectively. Total mass loss is 40%. The different mass losses can be represented schematically as follows:

$$Ni_2(L^5)\cdot 4H_2O \rightarrow Ni_2(L^5)\cdot 2H_2O \rightarrow Ni_2(L^5) \rightarrow 2NiO\cdot P_2O_5$$

It seems that after the total loss of water, the organic moiety decomposes, forming the end product, $2Nio\cdot P_2O_5$, requiring a theoretical mass loss of 40.46% [27–29, 32]. A similar result has also been postulated by Khramov et al. [33] for metal–HEDP complexes.

7. $Ni_2(L^6)\cdot 2H_2O$ complex (Fig. 7): Thermal degradation study of only $Ni_2(L^6)\cdot 2H_2O$ complex has been made. It is observed that two molecules of water were lost at 100 °C and mass loss on TG curve about 4.2% (theoretical, 4.34%). After that, no clear decomposition stage was detected on DTG curve. The decomposition pattern of TG curve shows that after the loss of two water molecules, the organic part starts decomposing. Final observed mass loss value of 42.5% (theoretical, 41.88%) is corroborated to the

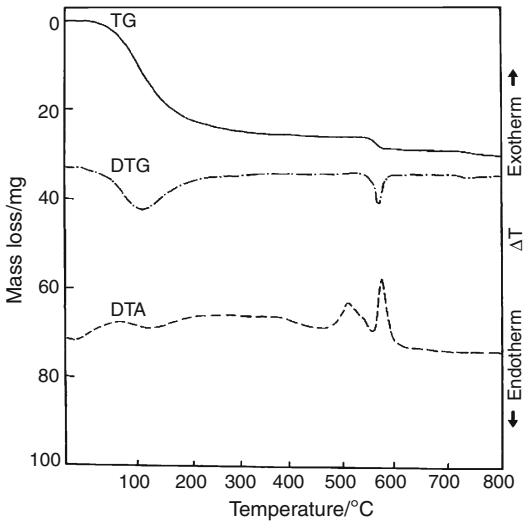

Fig. 6 Thermoanalytical curves of $Ni_2(C_8H_{18}N_2O_6P_2)\cdot 4H_2O$ (40 mg specimen)

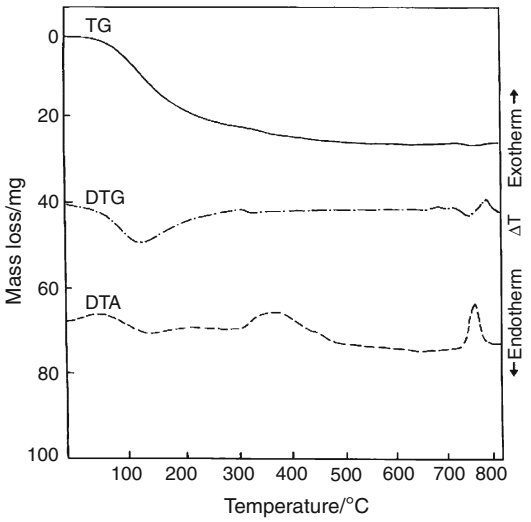

Fig. 8 Thermoanalytical curves of $Ni_5(C_9H_{18}N_3O_{15}P_5)\cdot 20H_2O$ (109.5 mg specimen)

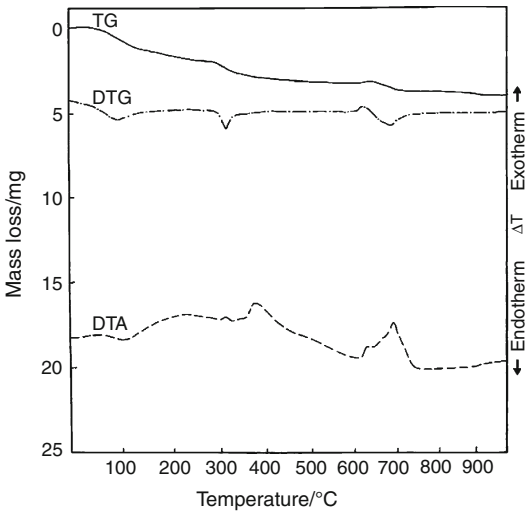

Fig. 7 Thermoanalytical curves of $Ni_2(C_{12}H_{18}N_2O_6P_2)\cdot 2H_2O$ (60 mg specimen)

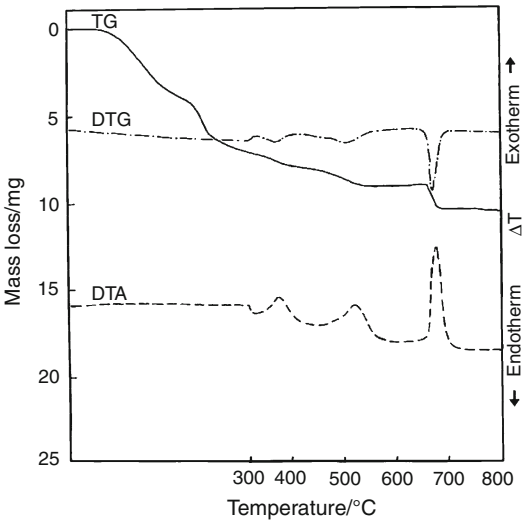

Fig. 9 Thermoanalytical curves of $Cu_5(C_3H_4NO_8P_2)_2\cdot 4H_2O$ (200 mg specimen)

formation of end product $2NiO\cdot P_2O_5$. Similar results have also been reported earlier [27–29, 32, 33].

8. $Ni_5(L^7)\cdot 20H_2O$ complex (Fig. 8): The thermo analytical curves of above complex clearly indicates that all the 20 water molecules were lost at 370 °C. However, the first endothermic peak was observed at 300 °C which corresponds to a mass loss of 27.3% due to the removal of 18 water molecules (theoretically required, 26.63%). At 370 °C, rest of the two water molecules are lost, the corresponding mass loss is 29.22% (theoretical, 29.59%). The decomposition of anhydrous metal phosphonate began after 370 °C and is characterized by the exothermic peaks observed at 520 and 680 °C and proceeded in steps. The total mass loss of 40.6% indicated the formation of nickel oxide and phosphorus pentoxide as the composition of the residue (theoretical mass loss being 40.11%).
9. $Cu_5(L^3)_2\cdot 4H_2O$ complex (Fig. 9): In this case, the first endothermic effect at 160 °C on the DTA curve corresponds to the loss of four water molecules. The second endothermic effect at 220 °C showed the loss of two NH_3 and two CO_2 molecules. The total mass loss (23%) indicates that the final product is $CuO\cdot P_2O_5$ (theoretical mass loss, 24.04%) [27–29, 32, 33].

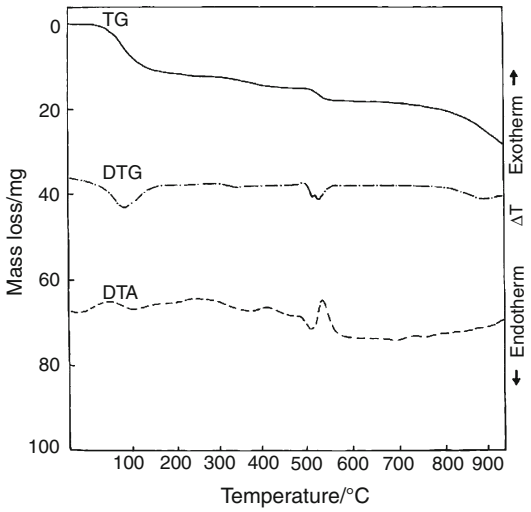

Fig. 10 Thermoanalytical curves of $Cd_5(C_9H_{18}N_3O_{15}P_5)\cdot 16H_2O$ (101.5 mg specimen)

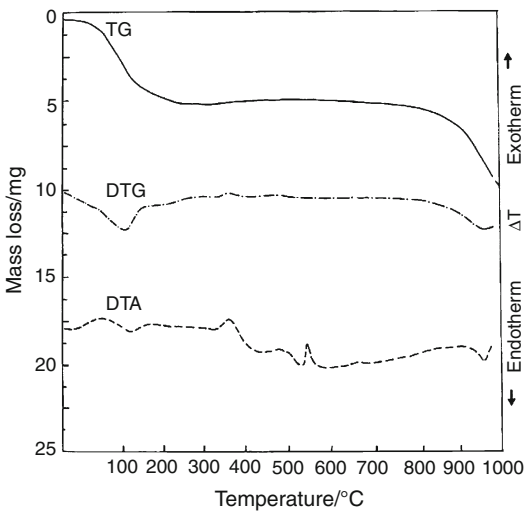

Fig. 11 Thermoanalytical curves of $Cd_5(C_{10}H_{23}N_3O_6P_2)\cdot 3H_2O$ (108 mg specimen)

10. $Cd_5(L^7)\cdot 16H_2O$ complex (Fig. 10): In this case, all the 16 water molecules were lost in four clear steps. The first endothermic peak at 110 °C on DTA curve shows that seven water molecules were lost and corresponding mass loss for which is 8.37% (theoretical, 8.91%). At 380 °C, the next four water molecules were lost (theoretical, 14.01%; observed, 14.28%). The third effect at 510 °C indicated the loss of another two water molecules. On TG curve, the loss in mass was 16.25%, theoretical being 16.55%. The loss of rest of the three water molecules is not indicated through a clear step. However, these three were lost at about 775 °C (observed loss in mass was 20.19%; theoretical, 20.38%). After the loss of all the water molecules, the organic part starts decomposing and the total mass loss of 29.16% indicated the formation of the end product cadmium oxide and phosphorus pentoxide which is also corroborated by theoretical mass loss (29.43%) for the formation of the end product.
11. $Cd_2(L^8)\cdot 3H_2O$ complex (Fig. 11): The thermo analytical curves of $Cd_2(L^8)\cdot 3H_2O$ complex shows loss of three water molecules up to 95 °C and corresponding mass loss is 8.74%, theoretical being 9.25%. After that, no clear steps on DTG curve could be detected. However, two exothermic peaks at 370 and at 540 °C were observed on DTA curve and corresponding mass losses are 18.98 and 18.51%, respectively. After the loss of three water molecules, the organic part starts decomposing. The total loss in mass on TG curve is 35.11% (theoretical, 35.44%) which is corroborated to the formation of end product cadmium oxide, and phosphorus pentoxide. Similar results have also been reported from these laboratories [27–29, 32] as well as Khramov et al. [33] for their rare earth metal phosphonates.

EPR spectral study [73, 74]

EPR measurement has been made for $Cu_5(L^3)_2\cdot 4H_2O$ complex ($Cu_5(ACEDP)_2\cdot 4H_2O$) using a powdered sample, which could provide only a value of g_{av} and does not give any hint about the individual $g_{\perp\perp}$ and g_1 values. The g_{av} value of the $Cu_5(ACEDP)_2\cdot 4H_2O(Cu_5(L^3)_2\cdot 4H_2O)$ complex was calculated to be 2.13 which deviates slightly from the free spin value. This deviation may be due to the covalent bonding. The g_{av} value also supports a tetragonally distorted structure as has also been suggested by Low [74].

Conclusions

All these complexes were insoluble in water as well as other common organic solvents and did not melt even up to 270–280 °C. The properties indicated them to be polymeric in nature. Polymeric/poly nuclear nature has also been established based on phosphoryl oxygen coordinated to metal atom, which is assigned from the IR data of metal derivatives. Stereochemistry of complexes were found to have hexa-coordinated and distorted octahedral geometry. EPR spectral study of some of the copper(II) complexes has been made and from this, these compounds have been found to be tetragonally distorted. The magnetic moments of the complexes have been found to be subnormal at room

temperature. These low magnetic moment values may be due to the presence of antiferromagnetism which can arise due to polymeric nature of the complexes, and thus bring the metal ions at distance close enough to interact or through super exchange via phosphonic acid or hydroxo bridges (in case of trivalent metal compounds). Aggarwal et al. have reported that due to the partial oxidation of the metal atom to the higher oxidation of the central metal atom to the higher oxidation state also, the lowering of magnetic moment value takes place. This possibility in case of cobalt(II) in the present investigation was ruled out because the magnetic moment of the complexes was not effected even when kept in air for long (10 to 30 days). The magnetic moments have decreased with decreasing temperature. A straight line was obtained when $1/\chi'M$ was plotted against temperature. Curie–Weiss law is also obeyed with the θ values ranging from 77 to –297 K. Thermal behaviour (TG, DTA and DTG) of some of the complexes of different series showed thermal degradation pattern and can be represented schematically as follows:

$$M_nL \cdot xH_2O \rightarrow M_nL \rightarrow nMO \cdot P_2O_5$$

Acknowledgements Thanks are due to C.S.I.R fellowships to Dr. B.V.R. Thanks are also due to Management of ALC for encouragement.

References

1. Delvin BRJ. Shell International Research Maats Chappis B.V. Brit. 11; 1978. p. 508, 772 (c, AO1N 9136).
2. Delvin BRJ Shell International Research Maats Chappis B.V. Brit. 74115; 1974. p. 15, 255.
3. Delvin BRJ Chem Abstr 1974;90:34989e.
4. Schindler N, Ploeger W, Ger Offen 1972;2048:913–18 (2,048,913 Appl P).
5. Schindler N, Ploeger W, Ger Offen. Chem Abstr;77:19799d.
6. Kabachnik MI, Medved TYa, Arkhipova OG, Dyatlova NM, Rudomino MV. Organophosphorus complexones. Russ Chem Rev. 1968;7:503–18.
7. Zablotna R, Zylicz E, Szot Z, Peskorska C, Anna G. Nukleonika 1977;22(8):703–11 (in English).
8. Zablotna R, Zylicz E, Szot Z, Peskorska C, Anna G (1978) Chem Abstr 88:59775h.
9. Balabukha VS, IrannikovAI, Razhitnaya LI, Razamovskii NC, Tikhonaya LI, Baranovskaya LM. In: Second European Congress on Radiation Protection, 1972; 1973 pp. 293–298 (in English).
10. Balabukha VS, IrannikovAI, Razhitnaya LI, Razamovskii NC, Tikhonaya LI, Baranovskaya LM. Chem Abstr 1974;80:45278q.
11. Ploger W, Schindler N, Wollmann K, Woras KN. Herstellung von 1-Aminoalkan-1,1-diphosphonsäuren. Z Anorg Allg Chem. 1972;389:119.
12. Lerch I, Kottler A German Patent no 1,002,355, Feb 14; 1957.
13. Lerch I, Kottler A. Chem Abstr 1959;53:21814c.
14. Kabachnik MI, Medved TYa, Kozlova GK, BalaBukhaVS, Senyavin MM, Tikhonova LI. Izv Akad Nauk SSSR Ctd Khim Nauk 1958;1070.
15. Kabachnik MI, Medved TYa, Kozlova GK, BalaBukhaVS, Mironova EA, Tikhonova. LI Izv Akad Nauk SSSR Ctd Khim Nauk 1959;53:3039h.
16. Kabachnik MI, Medved TYa, Kozlova GK, BalaBukhaVS, Mironova EA, Tikhonova LI. Izv Akad Nauk SSSR Ctd Khim Nauk 1958;1070.
17. Kabachnik MI, Medved TYa, Kozlova GK, BalaBukha VS, Mironova EA, Tikhonova LI. Izv Akad Nauk SSSR Ctd Khim Nauk 1960;651.
18. Kabachnik MI, Medved TYa, Kozlova GK, BalaBukhaVS, Mironova EA, Tikhonova LI. Izv Akad Nauk SSSR Ctd Khim Nauk 1967;1501.
19. Kabachnik MI, Medved TYa, Kozlova GK, BalaBukhaVS, Mironova EA, Tikhonova LI. Izv Akad Nauk SSSR Ctd Khim Nauk Chem Abstr 1959;53:3039f.
20. Kabachnik MI, Medved TYa, Kozlova GK, BalaBukhaVS, Mironova EA, Tikhonova LI. Izv Akad Nauk SSSR Ctd Khim Nauk Chem Abstr 1960;54:22329b.
21. Kabachnik MI, Medved TYa, Kozlova GK, BalaBukhaVS, Mironova EA, Tikhonova LI Izv Akad Nauk SSSR Ctd Khim Nauk Chem Abstr 1968;68:24798w.
22. Peck DR, Hudson D. Brit. 1,42,294 (Cl C07f).
23. Peck DR, Hudson D. Chem Abstr 1969;70:106650x.
24. Medved TYa, Rudomino MV, Mironova EA, BalaBukha VS, Kabachnik MI. Izv Akad Nauk Ser Khim. 1967;2:351–6. (Russian).
25. Rao BV. Ph.D thesis. Kurukshetra University, Kurukshetra; 1985.
26. Vogel AI. A text book of quantitative inorganic analysis. 7th ed. London: Longman; 1996.
27. Venkateswara Rao B, Puri DM. Iron(II) and iron(III) complexes of organophosphonic acids. Orient J Chem. 2009;25(1):85.
28. Palta N, Rao BV, Dubey SN, Puri DM. Organophosphonic acids as complexones. Part IV. Polymeric complexes of ethylenediamine-N,N′-bis(methylenephosphonic acid and phenylenediamine-N,N′-bis(methylenephosphonic acid). Indian J Chem. 1984;23A:397.
29. Palta N, Rao BV, Dubey SN, Puri DM. Ethylenediamine-N′,N′,N″,N″-tetrakis(methylenephosphonic)acid as complexing agent. Polyhedron. 1984;5:527.
30. Żurowska B, Mrozinski J, Ochocki J. Coordination properties of the diethyl 2-quinolilmethylphosphonate ligand with chloride and nitrate transition-metal salts. Mater Sci. 2007;25(4):1063–74.
31. Saad EA, Ramadan RM. Synthesis and characterization of some new organophosphonates and their adducts with some metal salts. Bull Chem Soc Jpn. 1989;62:3697–700.
32. Tusek-Bozic L, D'alpaos M, Curic M, Lycka A. Synthesis and Characterization of metallocyclic complexes of palladium(II) with monoalkyl (*alpha*-anilino-*N*-benzyl)phosphonates. Croat Chem Acta CCACAA. 2001;74(4):825–36.
33. Nash KL, Rogers RD, Ferraro J, Zhang J. Lanthanide complexes with 1-hydroxyethane-1,1-diphosphonic acid: solvent organization and coordination geometry in crystalline and amorphous solids. Inorgan Chim Acta 1998;269(2):211.
34. Ochocki J, Zurowska B, Mrozinski J, Kooijman H, Spek AL, Reedijk J. Synthesis, spectroscopy, and magnetic properties of transition-metal complexes with the diethyl 2-quinolylmethylphosphonate (2-qmpe) ligand—crystal structures of $[Ni(2\text{-qmpe})_4(H_2O)_2](ClO_4)_2$ and $[Mn(2\text{-qmpe})_4(H_2O)_2](ClO_4)_2$ showing unexpected O-binding of the qmpe ligands. Eur J Inorg Chem. 1998;2:169.
35. Scheinmann F, editor. An introduction to spectroscopy methods for the identification of organic compounds. Oxford: Pergamon Press; 1970.
36. Fujita J, Nakamoto K, Kobayashi M. Infrared spectra of metallic complexes II. The absorption bands of coördinated water in aquo complexes. J Am Chem Soc. 1956;78:3963.
37. Jani GR, Vyas KB, Franco Z. Preparation and antimicrobial activity of *s*-triazine hydrazones of 7-hydroxy coumarin and their metal complexes. E-Journal Chem. 2009;6(4):1228.

38. Reddy V, Patil N, Angadi SD. Synthesis, characterization and antimicrobial activity of Cu(II), Co(II) and Ni(II) complexes with O, N, and S donor ligands. E-J Chem. 2008;5(3):577–83.
39. Sengupta SK, Sahni SK, Kapoor RN. Mixed ligand complexes of ruthenium(III), rhodium(III), iridium(III) with dipicolinic acid and some mono basic bidentate nitrogen, oxygen donor ligands. Polyhedron. 1983;2:317.
40. Maurya RC, Chourasia J, Sharma P. Synthesis, characterization and 3D molecular modeling of some ternary complexes of Cu(II), Ni(II), Co(II), Zn(II), Sm(III), Th(IV) and UO_2(VI) with Schiff base derived from the sulfa drug sulfabenzamide and 1,10-phenanthroline. Indian J Chem. 2007;46A:1594–604.
41. Maurya RC, Sharma P, Sutra Dhar D. Synthesis, magnetic, and spectral studies of some mixed-ligand complexes of copper(II) involving diphenic acid and pyridine or aniline derivatives. Synth React Inorg Met Org Chem. 2003;33:669.
42. Kose DA, Gokce G, Gokce S, Uzun I. Bis(N,N-diethylnicotinamide) *p*-chlorobenzoate complexes of Ni(II), Zn(II) and Cd(II). J Therm Anal Calorim. 2009;95:247–51.
43. Dyer JR. Applications of absorption spectroscopy of organic compounds. New Delhi: Prentice Hall of India; 1978. p. 37.
44. Sharma R, Bansal KA, Nagar M. Transition metal complexes of cis-3,7-dimethyl-2,6-octadien-thiosemicarbazone: synthesis, characterization and biocidal studies. Indian J Chem. 2005;44A: 2255.
45. Souanya ER, Ismail EH, Mohamed AA, Milad NE. Preparation, characterization and thermal studies of some transition metal ternary complexes. J Therm Anal Calorim. 2009;95(1):253–8.
46. Syamal A, Maurya MR. Coordination chemistry of schiff base complexes of molybdenum. Coord Chem Rev. 1985;95:183.
47. Maurya RC, Mishra DD, Mukherjee S, Trivedi PK. Synthesis, magnetic and spectral studies of mixed-ligand derivatives of cobalt(II) and nickel(II)-β-diketonate and β-diketoesters with some potentially bi- and tri-dentate heterocyclic nitrogen donors. Synth React Inorg Met Org Chem. 1991;21:1107.
48. Lever ABP. Inorganic electronic spectroscopy. 2nd ed. New York: Elsevier; 1986.
49. Rogan J, Poleti D, Karanovic L, Bogdanovic G, Spasojevic-de Bire A, Petrovic DM. Mixed ligand Co(II), Ni(II) and Cu(II) complexes containing terephthalato ligands. Crystal structures of diaqua(2,2′-dipyridylamine) (terephthalato)metal(II)trihydrates (metal = cobalt or nickel). Polyhedron. 2000;19:1415.
50. Sharma HK, Chandra S, Gupta S. Synthesis and spectral studies of nickel(II) and cobalt(II) complexes of a twelve-membered and tetradentate macrocyclic ligand. Synth React Inorg Met Org Chem. 1997;27(8):1083.
51. Sivasankar B. Cobalt(II), nickel(II) and zinc(II) dicarboxylate complexes with hydrazine as bridged ligand: characterization and thermal degradation. J Therm Anal Calorim. 2006;86(2):385–92.
52. Vikram L, Shanthakumar D, Ragul R, Sivasankar B. Spectral and thermal studies on new hydrazinium metal sulfite dehydrates. J Therm Anal Calorim. 2007;89(2):521–4.
53. Yeşilel OZ, Ölmez H. Spectrothermal studies of 1,10-phenanthroline complexes of Co(II), NI(II), Cu(II) and Cd(II) orotates. J Therm Anal Calorim. 2006;86(1):211–6.
54. Yeşilel O, Ölmez H. Syntheses and spectrothermal studies of triethanolamine complexes of Co(II), Ni(II), Cu(II) and Cd(II) squarates. J Therm Anal Calorim. 2007;89(1):261–5.
55. Modi CK, Patel SH, Patel MN. Transition metal complexes with uninegative bidentate Schiff base: synthetic, thermal, spectroscopic and coordination. J Therm Anal Calorim. 2007;87(2): 441–8.
56. Kose DA, Gokce G, Gokce S, Uzun I. Bis(N,N-diethylnicotinamide)*p*-chlorobenzoate complexes of Ni(II), Zn(II) and Cd(II) synthesis and characterization. J Therm Anal Calorim. 2009; 95:247.
57. Cotton FA, Wilkinson G, Murillo CA, Bochmann M. Advanced inorganic chemistry. 6th ed. New York: Wiley; 1999.
58. Maurya RC, Sharma P, Roy S. Synthesis and characterization of some mixed-ligand picrate complexes of nickel(II) involving heterocyclic nitrogen donors. Synth React Inorg Met Org Chem. 2003;33:683.
59. Ferenc W, Bocian B, Sarzyński J. Thermal, spectral and magnetic behaviour of 2,3,4-trimethoxybenzoates of Mn(II), Co(II), Ni(II) and Cu(II). J Therm Anal Calorim. 2006;84(2):377–83.
60. Ferenc W, Cristóvão B, Sarzyński J. Complexes of Mn(II), Co(II), Ni(II), Cu(II) and Zn(II) with 4-chloro-2-methoxybenzoic acid anion. J Therm Anal Calorim. 2006;86(3):783–9.
61. Dianzhong F, Bo W. Complexes of cobalt(II), nickel(II), copper(II), zinc(II) and manganese(II) with tridentate Schiff base ligand. Trans Met Chem. 1993;18:101.
62. Dutta RL, Syamal A. Elements of magnetochemistry. 2nd ed. New Delhi: Affiliated East-West Press Pvt. Ltd.; 1993. p. 57, 107.
63. Dubey RK, Mishra CM. Synthesis, reactions, spectral and magnetic studies of chloro-[2-*o*-hydroxyphenyl)]-benzimidazolato]-cobalt(II). Indian J Chem. 2006;45A:2203–8.
64. Aggarwal RC, Bala R, Prasad RL. Ternary complexes of oxovanadium(IV), manganese(II), cobalt(II), nickel(II), copper(II) and zinc(II) with 2-aminobenzoic acid and 1-nitroso-2-naphthol. Indian J Chem. 1983;22A:955.
65. El-Dissouky Ali, Mohamed GR, Refaat LS. Metal chelates of heterocyclic nitrogen containing ketones, XIII. Cobalt(II), nickel(II) and palladium(II) complexes of 2-picolyl- and 2-lutidylmethyl ketones. Trans Met Chem. 1984;9:23.
66. Andrew JE, Ball PW, Blake VB. Binuclear cobalt(II) and nickel(II) complexes of dihydrazinophthalazine and dipyridylpyridazine: the dependence of superexchange on electronic configuration. Chem Commun 1969;143.
67. Ball PW, Blake AB. Magnetic properties of polynuclear complexes. Part I. Superexchange in some binuclear nickel(II) complexes. J Chem Soc 1969;1415–22.
68. Bhatnagar SS, Khanna ML, Nevgi MB. Phil Mag 1938;25.
69. Figgis BN, Lewis J. In: Cotton FA, editors. Progress Inorgan Chem. New York: Wiley-lnterscience; 1964. p. 188.
70. Palta N. Ph.D thesis. Kurukshetra University, Kurukshetra; 1964.
71. Figgis BN. Introduction to ligand fields. New Delhi: Wiley Eastern; 1966.
72. Manhas BS, Kalia SB, Sardana AK, Kaushal G. Magnetic and spectroscopic characterization of copper(II) chlorobenzoate adducts with substituted piperidines. Indian J Chem. 2005;44A: 1576–81.
73. Low W Paramagnetic resonance in solids. Suppl 2. In: Seity F, Turnbull D, editors. Solid State Phys. New York: Academic Press; 1960. p. 92.
74. Abraham A, Bleaney B. Electron paramagnetic resonance of transition metal ions. Oxford: Clarendon Press; 1970.